

## A Study on Accuracy of Micro-Holes Drilled in Ti-6Al-4V Alloy by Using Electrical Discharge Machining Process

Magdalena Machno<sup>1\*</sup>, Marcin Trajer<sup>2</sup>, Wojciech Bizoń<sup>3</sup>, Adrian Czeszkiewicz<sup>4</sup>

<sup>1</sup> Department of Rail Vehicles and Transport, Faculty of Mechanical Engineering, Cracow University of Technology, al. Jana Pawła II 37, 31-864 Cracow, Poland

<sup>2</sup> Division of Surface Engineering, Faculty of Materials Science and Engineering, Warsaw University of technology, ul. Wołoska 141, 02-507 Warsaw, Poland

<sup>3</sup> Department of Production Engineering, Faculty of Mechanical Engineering, Cracow University of Technology, al. Jana Pawła II 37, 31-864, Cracow, Poland

<sup>4</sup> Łukasiewicz Research Network – Institute of Aviation, al. Krakowska 110/114, 02-256 Warsaw, Poland

\* Corresponding author's e-mail: magdalena.machno@pk.edu.pl

### ABSTRACT

Thermophysical properties of the Ti-6Al-4V titanium alloy make it difficult to process with electro discharge machining (EDM) process. The aim of this experimental work was to investigate manufacturing of micro-holes in titanium alloy by means of EDM. Further investigation the accuracy of drilled holes was performed in order to improve the EDM drilling method in this alloy. As a part of the research, the impact of four EDM process parameters on performance factors such as: material removal rate (MMR), linear tool wear (LTW) was verified in parallel to accuracy metrics of the micro-hole: radial overcut (ROC), cylindricity (CYL), recast layer thickness (RLT). The analysis of the obtained relationships showed that the properties of the Ti-6Al-4V alloy, such as low thermal conductivity, and low electrical conductivity significantly affect the EDM process efficiency. It is clearly visible through increased electrode wear, as well as the accuracy and quality reduction of the drilled holes. When analyzing the accuracy of the hollow micro-holes, it was observed that the highest current amplitude resulted in a smaller amount of microcracks in the layer around the hole entrance. The optimal process parameters to obtain a satisfactory geometry of micro-holes have been found such as: current amplitude 3.33–4.65 A, pulse time duration 550–1000  $\mu$ s, open voltage 100 V, and tool rotation speed 300 rpm.

**Keywords:** micro-hole, EDM-drilling, difficult-to-cut material, Ti-6Al-4V alloy.

### INTRODUCTION

Titanium alloys, thanks to their strength and thermophysical properties combined with relatively low density have been broadly used for aviation, automotive and medical elements. The most desirable properties of these alloys are low modulus of elasticity, and excellent corrosion resistance, high strength-to-weight ratio, and good resistance to creep, fatigue, and biocompatibility [1,2]. However, due to these properties of titanium alloys, their processing by conventional methods which most often are used for the production of parts, is very difficult [3]. For this reason,

energy-based techniques such as EDM [4] are used for machining titanium alloys. Also according to [5], EDM is one of the frequent choices of the technique used for thin and complex shapes manufacturing within hard materials.

In the case of the production of parts in the above-mentioned industries, a particular challenge is the effective production of micro-holes in turbine blades, fuel injectors, medical equipment, cutting tools. These holes are characterized by a geometry with a diameter of 0.15–3 mm with a length-to-diameter ratio of over 150: 1 [6]. Manufacturing of long micro-holes with diameters smaller than 1 mm [7] by means of EDM is an

area which is still being developed and improved. This is due to the difficulty of providing sufficient flushing to the machining area. That happens especially when the hole is already drilled to a certain depth. greater wear of the tool electrode (in the micro-EDM process, the tool wear can reach up to 100% [8]), collecting at the bottom of the hole during the process of eroded particles, which are difficult to remove [9,10]. The mentioned debris contributes to the distortion of the hole geometry as well as to the faster wear of the tool electrode [11].

The machining of titanium alloys with the EDM process has been studied for many years. The analyzed process parameters include the length of the pulse time, the length of the pause time, the current amplitude, the operating voltage, the rotation of the working electrode, and flushing pressure. Moreover, the influence of the type of dielectric, the type of material of the working electrode and the shape of the working electrode are analyzed [12]. The influence of EDM process parameters during the treatment of Ti-6Al-4V titanium alloy was analyzed in [13]. The authors reported that the wear of the working electrode during titanium alloy machining is related to carbide formation at the bottom surface of the tool electrode. The study investigated the impact of EDM parameters such as pulse time length ( $t_{on}$ ) and current amplitude ( $I$ ). As a result, the maximum material removal rate ( $\sim 2.71 \text{ mm}^3/\text{min}$ ) for  $I = 25 \text{ A}$ ,  $t_{on} = 200 \mu\text{s}$ , surface roughness of the EDMed sample varies from 2.26 to 4.08  $\mu\text{m}$ , and the lowest energy input (for  $I = 6 \text{ A}$ ,  $t_{on} = 50 \mu\text{s}$ ) reaches minimum surface roughness ( $Ra \sim 2.26 \mu\text{m}$ ). However, the authors note that further research is still needed on the efficiency of the EDM process when machining titanium alloys. An interesting work on the improvement of EDM machining of titanium alloys is the work [14]. The Authors proposed a new kind of compound dielectric with appropriately selected processing parameters. It has been shown that new kind of compound dielectric with appropriately selected parameters provides 1.5 times faster processing than when using distilled water and 5 times faster than when using kerosene as dielectric fluid. Also obtained for the new dielectric was a lower surface roughness  $Ra$  by approx. 14% than when using distilled water.

Many researchers conduct experiments aimed at broadening the knowledge of making micro-holes in titanium alloys by means of EDM. In [15] the influence of capacitance, current, pulse

on time and off time over technological variables on the material removal rate, electrode wear rate, overcut and taper were investigated. It was shown that overcut and taper were mostly influenced by the current, followed by capacitance, pulse on time, and pulse off time. In addition, it was observed that higher electrode wear caused a greater overcut. Author explained it by the conical shape of the electrode. It was also reported that use of smaller values of both current peak and pulse on time resulted in better topographical conditions of micro-holes. However, even with mentioned above findings the geometry of obtained micro-holes was not satisfactory.

In order to find the appropriate setup of the EDM process parameters, optimization of the parameters is also performed for micro-holes drilled in the titanium alloy. In [16] optimization of the parameters was performed using the TOPSIS fuzzy technique to simultaneously optimize the material removal rate and overcut. The optimal parameters of the EDM process were found as follows: capacitance 1000 pF, voltage 100 V, pulse on time 100  $\mu\text{s}$ , and tool rotation 500 rpm.

Moreover, the research focuses not only on the selection of appropriate process parameters but also on the influence of other factors. In [17] the influence of various working fluids such as EDM oil – DEF-92, deionized water or Cu powder mixed with deionized water on MMR, LTW, diametral overcut, and taper was tested. The analysis of the results showed that the treatment with deionized water allowed to achieve of the minimum thickness of the white layer compared to other dielectric fluids. Moreover, the increase of peak current resulted in an increase in the material removal rate, regardless of the dielectric used. An improvement in a diametral overcut and taper was obtained when the current amplitude range was set as follows: 0.5–1.0 A for treatment with deionized water, 1.5–2.0 A for Cu powder mixed with deionized water. However, still, both the quality of the boreholes and the performance parameters could be improved. The authors indicate the need to investigate the influence of other parameters of the EDM process.

Accordingly, there is a visible need to improve the efficiency of the EDM process when making micro-holes in titanium alloy. For this purpose, further research into the process itself and its phenomena are necessary. It is also necessary to develop new technological solutions that would improve the efficiency factors of the EDM

process and, at the same time, the dimensional and shape accuracy of the micro-holes. Moreover, the micro-erosion technique in titanium alloys (especially long holes) is still being developed [18]. There is also a tendency to make smaller and smaller diameter micro-holes. This results in the adoption of new parameter and the use of new technological solutions (e.g. a better method of rinsing the treatment area, using electrodes coated with non-conductive layers). Hence, it is assumed that the research on electro-discharge machining carried out in this article is still a new and not fully explored research area.

The article presents the results of the research on electro-erosion micro-drilling in the Ti-4V-6Al titanium alloy. The aim of the results analysis was to extend knowledge regarding the phenomena present during the EDM of the selected titanium alloy. Moreover, goal of the study was to develop parameters improving the process efficiency and the geometry of the micro-holes. For this purpose, an analysis of the influence of EDM process parameters (current amplitude, operating voltage, pulse time length, rotational speed of the working electrode) on performance factors (material removal rate and linear tool wear) and the accuracy of the micro-hole (radial overcut, cylindricity, recast layer thickness) was conducted. Observations of micro-holes using a scanning electron microscope (SEM) and backscattered electrons (BSE) allowed more accurate observation of holes entrance surface.

## MATERIALS AND METHODS

### Materials used

The experimental research used the Ti-6Al-4V alloy as the workpiece material, which belongs to the group of  $\alpha + \beta$  martensitic two-phase alloys. The dimensions of the workpiece sample were 30×25×10 mm. The micro-holes were drilled with a copper tube-electrode with an outer diameter of 400  $\mu\text{m}$  and inner channel diameter of 215  $\mu\text{m}$ . Selected materials are most commonly used for jet engines turbomachinery elements which was the determining factor for its

choice. Properties of this titanium alloy, such as hardness – 36 HRC, fatigue strength – 510 MPa, yield tensile strength – 870 MPa, modulus of elasticity – 13.8 GPa, make it the choice for the material of parts in the aviation industry [19]. According to [20], this kind of tool electrode is the best tool for electrical discharge drilling of micro holes. Table 1 presents the chemical composition of the Ti-6Al-4V alloy. For the EDM process, the thermophysical properties of the workpiece material and the working electrode have a significant influence on the process. For this reason, Table 2 presents selected properties of the machined titanium alloy and copper electrode.

### Experimental procedure

Experimental studies of electrical discharge drilling were carried out on the test stand used for EDM and electrochemical machining (ECM).

During the EDM research, the workpiece and tool electrode was connected to an electrical pulse generator. Between the electrodes, there is a narrow interelectrode gap with starting setup equal to  $S_0$  (see in Figure 1b). Electrode was mounted in to the spindle, which rotated with constant RPMs. During the tests, the ceramic tool guide was used, which minimized the runout of the electrode. The test showed that the electrode runout was very slight and amounted to  $\sim 0.01$  mm, which proves the functionality of this method. The working fluid was flushed down under pressure to the gap area through the tube-electrode channel. Below the scheme of test stand and the experimental setup are shown, respectively in Figure 1a and Figure 1b.

During the test the constant conditions was applied such as:

- initial interelectrode gap,  $S_0 = 50 \mu\text{m}$  (see in Figure 1),
- drilling time of each hole: 45 min (or shorter in the case where the through hole was obtained faster),
- pulse off duration, equalled pulse on duration,
- inlet working fluid pressure: 7 MPa,
- working fluid: deionized water.

The experimental study results were used to determine the influence of selected parameters of

**Table 1.** Typical chemical composition of Ti-6Al-4V alloy (wt. %)

Chemical element	Titanium	Aluminum	Vanadium	Iron	Oxygen	Hydrogen
wt. (%)	Balance	6	4	< 0.25	< 0.2	< 0.015

**Table 2.** Thermophysical properties of Ti-6Al-4V alloy and copper tool [21]

Property (unit)	Material	
	Ti-6Al-4V alloy	Copper tool
Density (g/cm <sup>3</sup> )	4.43	8.9
Melting point (°C)	1660	1084
Electrical resistivity (Ωcm)	178 × 10 <sup>-6</sup>	16.78 × 10 <sup>-9</sup>
Thermal conductivity (W/m·K)	6.7	401

the EDM process on the process performance factors, as well as to test the dimensional and shape accuracy of micro-holes. The influence of four process parameters such as

- open voltage,  $U$  (V)
- pulse-on duration,  $t_{on}$  (μs)
- current amplitude,  $I$  (A)
- tool rotation speed,  $N$  (rpm)

On the other hand, the performance factors were:

- material removal rate, MRR (μm/s)
- linear tool wear, LTW (%)

and factors characterizing the geometry of the holes:

- radial overcut, ROC (μm)
- cylindricity, CYL (mm),
- recast layer thickness, RLT (μm).

The resulting factors were determined as follows:

- the material removal rate (MRR) was calculated from the following equation:

$$MRR (\mu\text{m/s}) = \text{hole depth}/\text{drilling time}, \quad (1)$$

where the hole depth was determined as the value of the tool electrode immersion from the initial workpiece surface.

- the linear tool wear (LTW) was calculated according to the formula:

$$LTW (\%) = \frac{\text{shortening of the tool electrode}}{\text{hole depth}}, \quad (2)$$

To determine the shortening of the tool electrode, the contact point of the electrode with the workpiece material surface was measured before each drilling test. The coordinates of the contact point were checked; then, after drilling, the tool electrode was re-positioned at the contact point and procedure was repeated. The difference between the Z-axis coordinate value from the contact point before and after processing was the shortening value of the tool electrode.

- the radial overcut (ROC) was calculated according to the below formula:

$$ROC (\mu\text{m}) = \frac{(\text{entrance diameter of hole} - \text{diameter of the tool electrode})}{2}, \quad (3)$$

- cylindricity, CYL (mm). The measurement of the holes was performed using the optical scanning method. The system Alicona Infinite Focus G5 (Alicona Imaging GmbH, Raaba / Graz, Austria) was used for scanning.

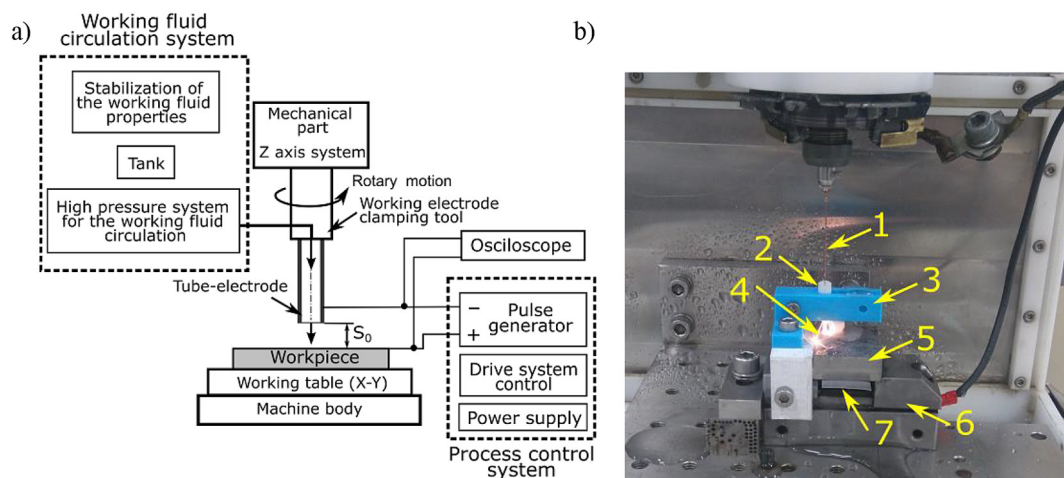


**Figure 1.** (a) Scheme of the EDM-drilling test stand; (b) The experimental setup of the electrodes guiding system, where: 1 – tool electrode, 2 – ceramic tool guide, 3 – tool guide attachment, 4 – sparks, 5 – workpiece material, 6 – clamp, 7 – technological pad

The system is equipped with a lens dedicated to scanning holes. The scanned hole entry (or exit) surface is transferred as a STP file to the GOM Inspect software. In this tool, a cylinder is automatically matched to each of the inlet and outlet cross sections. Knowing the height of the sample, cylindricity we can determined.

- recast layer thickness, RLT ( $\mu\text{m}$ ). Before measuring the thickness of the white layer, the sample was prepared appropriately (Figure 2). Then the workpiece was ground to remove the appropriate layer of material from the outer surfaces of the holes. During polishing, the polishing pad was poured with a hydrogen peroxide solution of  $\text{H}_2\text{O}_2$ . After the sample was polished, and to reveal the microstructure, an etching reagent of Krolls was applied.



Figure 2. Prepared sample to measure the recast layer

The surface etching time was approximately 5-6 seconds. Finally, the sample was washed with water and alcohol and dried. Then, the thickness of the heat affected zone around the entrance was measured. The same microscope was used for measurement as was used for the measurement of cylindricity. The measurement of the thickness of the white layer was made at eight points (Figure 3), and an average value was calculated from the obtained values.

Table 3 shows used process parameters and their levels. In case of open voltage parameter, its value changes in 60–120 V range with 20 V step. From that four variable values were used, such as 60; 80; 100 and 120 V. For the “0” level, the estimated values of the open voltage were rounded and closed to the higher value, therefore more tests with 100 V were used in the adopted test plan.

In the experimental research, the values of input parameters were adopted to allow stable and repeatable electrical discharge machining tests. The experimental investigation was performed based on the adopted study plan (see Table 4). The average values of the resulting factors, calculated based on formulas 1–3. The experimental tests were carried out according to the theory of the experiment using a rotatable study plan that included 31 experiments. The experimental tests consist of 26 various tests and five repetitions in the centre of the investigation plan (in Table 4 marked as C – the 27 tests with the mean value of

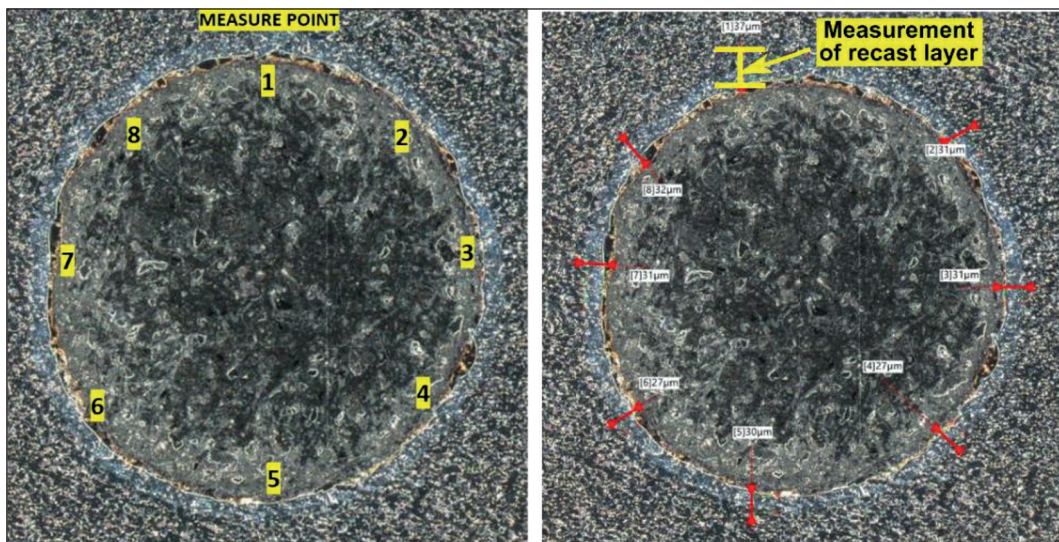


Figure 3. Method of measuring the thickness of the recast layer

**Table 3.** Process parameters and their levels

Parameter	Values Range	Levels				
		-2	-1	0/+1	+2	
<i>U</i> (V)	60–120	60	80	100	120	
<i>t<sub>on</sub></i> (μs)	100–1000	100	325	550	775	1000
<i>I</i> (A)	2.00–4.65	2.00	2.66	3.33	3.99	4.65
<i>N</i> (rpm)	100–500	100	200	300	400	500

**Table 4.** Design matrix and experimental results

Exp. Run	Parameters				Responses				
	<i>U</i> (V)	<i>t<sub>on</sub></i> (μs)	<i>I</i> (A)	<i>N</i> (rpm)	MRR (μm/s)	LTW (%)	ROC (μm)	CYL (mm)	RLT (μm)
1	80	325	2.66	400	5.59	13.23	117	0.063	23.96
2	80	325	2.66	200	4.15	6.14	123	0.057	24.36
3	80	325	3.99	200	22.94	13.01	83	0.050	27.03
4	80	325	3.99	400	24.51	9.75	103	0.063	26.62
5	80	775	2.66	200	8.20	8.43	111	0.056	32.44
6	80	775	2.66	400	16.53	9.00	77	0.044	32.03
7	80	775	3.99	400	15.87	9.30	123	0.064	34.69
8	80	775	3.99	200	11.43	9.63	113	0.077	35.10
9	100	325	2.66	200	9.70	7.31	101	0.047	23.50
10	100	325	2.66	400	8.95	7.12	108	0.047	23.09
11	100	325	3.99	400	18.66	6.92	106	0.052	25.75
12	100	325	3.99	200	15.22	4.45	112	0.048	26.16
13	100	775	2.66	400	9.77	5.98	110	0.050	31.16
14	100	775	2.66	200	9.81	14.30	112	0.060	31.57
15	100	775	3.99	200	24.81	12.49	108	0.059	34.23
16	100	775	3.99	400	21.74	16.24	113	0.075	33.83
17	60	550	3.33	300	13.61	15.28	88	0.058	32.18
18	120	550	3.33	300	8.50	14.48	245	0.068	29.58
19	100	100	3.33	300	18.32	11.15	65	0.036	19.39
20	100	1000	3.33	300	10.19	14.71	103	0.060	35.53
21	100	550	2.00	300	5.52	12.36	87	0.044	29.12
22	100	550	4.65	300	29.67	16.19	120	0.056	34.43
23	100	550	3.33	300	17.76	12.17	99	0.068	29.96
24	100	550	3.33	300	9.31	4.32	122	0.055	29.96
25	100	550	3.33	100	9.53	6.63	151	0.086	25.87
26	100	550	3.33	500	23.47	9.67	105	0.068	25.05
27(C)	100	550	3.33	300	11.40	13.61	107	0.052	29.96

repetitions). As a result of the experimental test, 31 through micro-holes were drilled.

To determine the influence of the input parameters on the process’s performance, Matlab software was employed. The “regstats” option was used to determine the function of the test object and calculate the resulting values. A second-degree polynomial (with constant, linear, and square terms) was used as the regression function. The following equations (4) – (8) were obtained:

$$\begin{aligned}
 \text{MRR } (\mu\text{m/s}) = & 5.80 + 0.29 U - 0.0079 t_{on} - \\
 & - 9.09 I - 0.03 N - 0.002 U^2 + \\
 & + 10^{-5} \times 0.59 t_{on}^2 + 2.6 I^2 + 10^{-5} \times 0.86 N^2,
 \end{aligned} \tag{4}$$

$$\begin{aligned}
 \text{LTW } (\%) = & 81.03 - 1.28 U - 0.009 t_{on} - \\
 & - 13.41 I + 0.38 N + 0.007 U^2 + \\
 & + 0.00001 t_{on}^2 + 2.19 I^2 - 0.00006 N^2,
 \end{aligned} \tag{5}$$

$$\begin{aligned} \text{ROC } (\mu\text{m}) = & 619.9 - 13.05 U + 0.13 t_{on} + \\ & + 11.95 I - 0.37 N + 0.08 U^2 - 0.0001 ton^2 - \\ & - 1.15 I^2 + 0.0005 N^2, \end{aligned} \quad (6)$$

$$\begin{aligned} \text{CYL } (\text{mm}) = & 0.06 - 0.001 U + 0.00008 t_{on} + \\ & + 0.04 I - 0.0003 N + 10^{-5} \times 0.07 U^2 - \\ & - 10^{-6} \times t_{on}^2 - 0.005 \times I^2 + 10^{-6} \times N^2. \end{aligned} \quad (7)$$

$$\begin{aligned} \text{WLT } (\mu\text{m}) = & 20.82 - 0.15 U + 0.032 t_{on} - \\ & - 4.9 I + 0.07 N + 0.001 U^2 - \\ & - 0.00001 t_{on}^2 + 1.04 I^2 - 0.00011 N^2 \end{aligned} \quad (8)$$

Analysis of the results shows that the values of the R-squared statistic ( $R^2$ ) for material removal rate, the linear tool wear, radial overcut, and cylindricity were 0.69, 0.37, 0.60, 0.59, and 0.71, respectively. Differences between the R-squared statistic and the adjusted R-squared statistic are smaller than 0.2. The high value of the coefficient  $R^2$  (near value 1) for MRR shows that the data of the regression model are very close to the experimental data. The lower value of the  $R^2$  coefficient for LTW is the result of analysing five input parameters as a response factors and smaller differences between obtained result. For all developed regression models the F statistic indicates that the

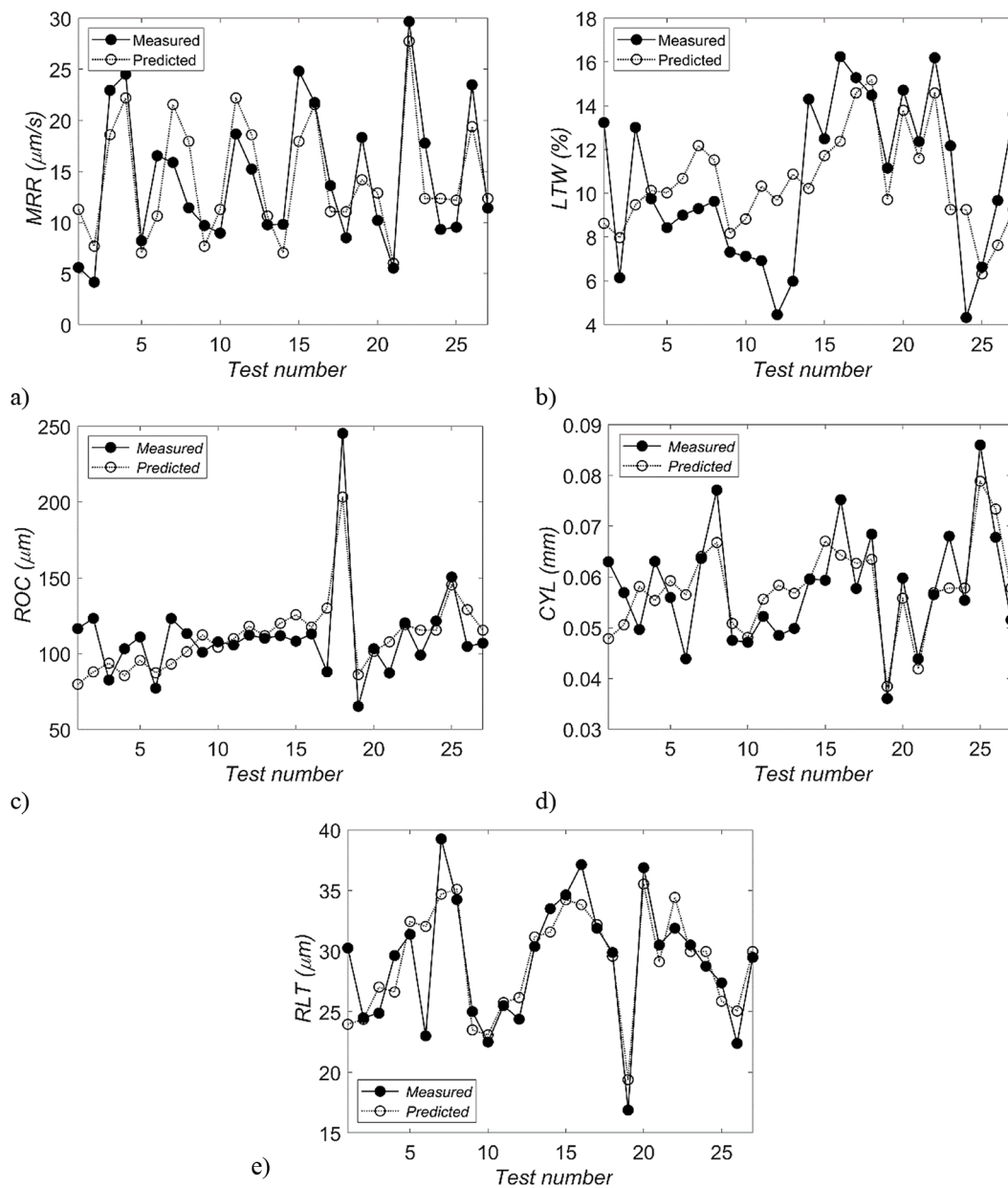


**Figure 4.** Comparison of measured and predicted values for a) material removal rate (MRR); b) linear tool wear (LTW); c) radial overcut (ROC); d) cylindricity (CYL); e) recast layer thickness (RLT)

p-values are less than 0.5, which confirms that the models obtained are statistically significant. Figure 4a–e. shows comparisons between the results of experimental studies and the values calculated based on the developed regression models for MRR, LTW, ROC, CYL, and RLT.

## RESULTS AND DISCUSSION

### Effect of EDM Parameters on MRR and LTW

MRR is one of the most important performance parameters of the EDM process [22]. This is due to the fact that it is key factor responsible for duration of manufacturing processes. Continuous search for less and less expensive processes leads need for improvements in efficiency of the EDM process, which is still much slower than the conventional machining and other nonconventional machining (e.g., electrochemical machining).

The MRR is mostly influenced by process parameters such as the current amplitude and the length of the pulse time, which determine the amount of energy of a single discharge and the time of its delivery [23]. However, in this case, the current amplitude has the greatest influence on the MRR. That is due to low thermal conductivity of the titanium alloy. Increased pulse on-time, what translates in to longer energy supply to the workpiece material, does not result in MRR increase (see in Figure 5). The workpiece material heats up slower and higher pulse time values did not significantly increase the MRR. Thus, the highest obtained MRR values (about 25  $\mu\text{m/s}$ )

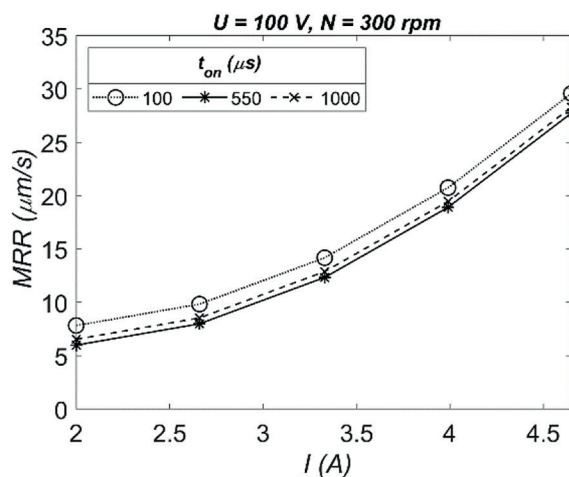


Figure 5. Effect of current amplitude ( $I$ ) and pulse on time ( $t_{on}$ ) on material removal rate (MRR)

were for the highest current value,  $I = 4.65 \text{ A}$ , and for all used pulse on time MRR had similar level.

In the EDM process, wear of the working tool electrode is also an important performance factor [22]. The consumption of electrodes in the process in the case of micro-machining can be up to 100%, which significantly increases the costs of the process. In the conducted research, the linear wear of tool electrode (LTW) was in the range of 10-20% (Figure 6). However, the holes were drilled to a depth of 10 mm. The analysis showed that, up to the 3.83 A current amplitude, the LTW was constant (approx. 10% with the applied pulse time length of 100 and 550  $\mu\text{s}$ ), and approx. 15% with the applied pulse time duration of 1000  $\mu\text{s}$ . While above of 4.00 A current amplitude, LTW increased. The highest LTW (approx. 20%) occurred for  $I = 4.65 \text{ A}$  and  $t_{on} = 1000 \mu\text{s}$ . This is related to the greater amount of energy in a single discharge pulse, which also removes more material along the length of the working electrode. Compared to titanium alloys, copper is a very good thermal conductor therefore the higher energy of a single discharge the higher consumption of the electrode material occurs.

Also, higher LTW occurred due to the transfer of heat from the treatment area to the electrode material, causing its increased wear. The properties of the Ti-6Al-4V titanium alloy contributed to this, are low thermal conductivity, low electrical conductivity and low melting point. These properties also made the drilling process more difficult. For the shorter impulse time used ( $t_{on} = 100 \mu\text{s}$ ), there were short-circuits and flat impulses in the process (Figure 7a). The short circuits only caused wear on the working electrode. Use of  $t_{on}$

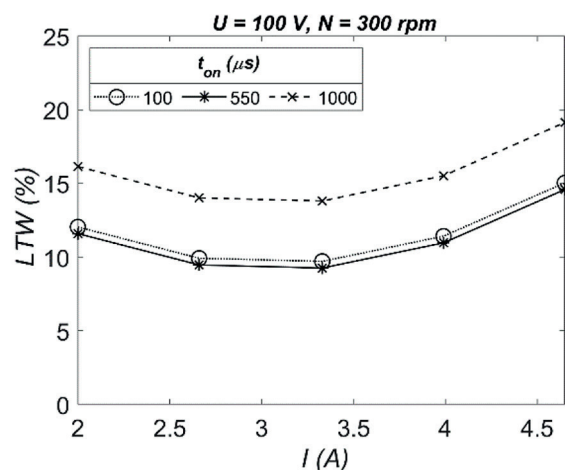
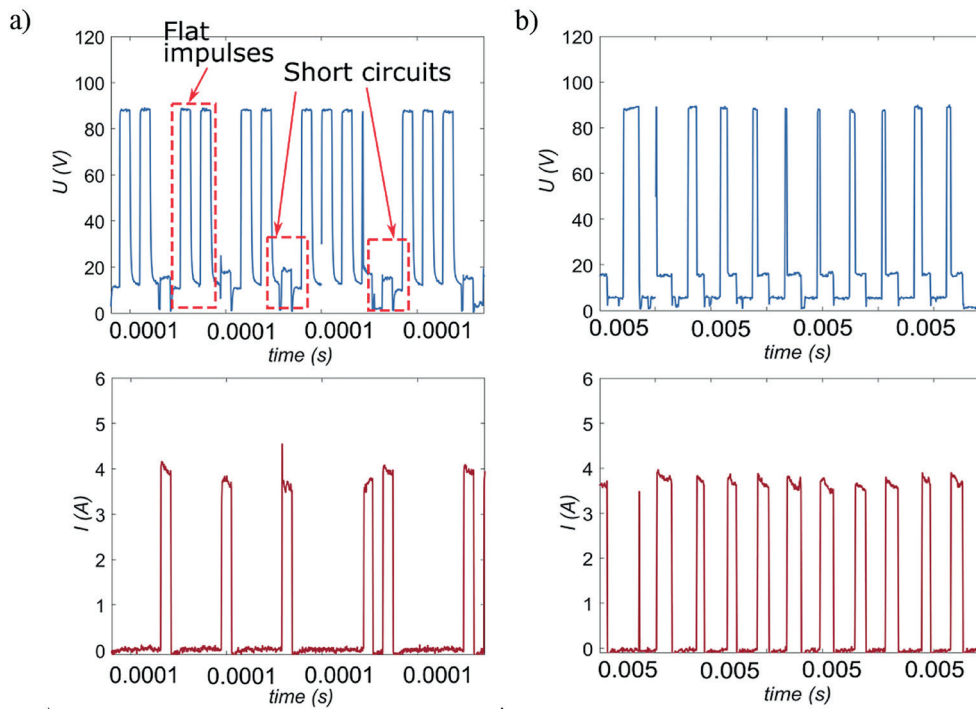
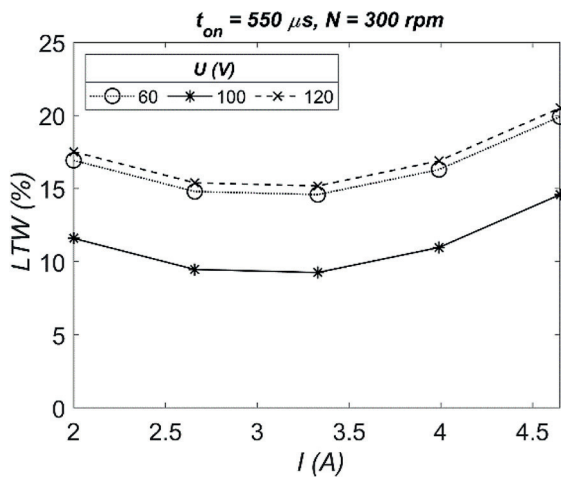


Figure 6. Effect of current amplitude ( $I$ ) and pulse on time ( $t_{on}$ ) on the linear tool wear (LTW)



**Figure 7.** The voltage and current waveforms for using of the pulse duration: a) 100  $\mu$ s and b) 550  $\mu$ s; constant parameters:  $I = 3.33$  A,  $U = 100$  V,  $N = 300$  rpm



**Figure 8.** Effect of current amplitude ( $I$ ) and open voltage ( $U$ ) on LTW

equal or greater to 550  $\mu$ s ensured occurrence of proper electrical discharges (Figure 7b). Hence, for  $t_{on} \geq 550 \mu$ s, the electrode wear resulted from the correct course of the drilling process.

Moreover, the analysis of the influence of the working voltage  $U$  on the linear wear of the electrode showed that the most optimal (providing a stable EDM-drilling process)  $U$  value, which results in lower electrode wear (at the level of approx. 10%), was 100 V (Figure 8).

The influence of the working voltage on the LTW was different. The recorded current and

open voltage waveforms for  $U = 60$  V (Figure 9a) and  $U = 120$  V (Figure 9b) indicate the occurrence of a short circuits, flat impulses, and arc discharges ( $I > 4$  A). These phenomena contribute to the unstable process and the increased wear of the working electrode, as shown in the Figure 6.

On the other hand, the recorded  $I(t)$  and  $U(t)$  waveforms during the use of  $U = 100$  V (Figure 10) show that the correct electrical discharges occurred in the process in the majority of cases. The above-described observations may result from use of deionized water as the working liquid what promoted creation of an appropriate electrical discharges. It is due to high value of the open voltage needed to insulation barrier of dielectric, in this case the value is 100 V. Deionized water has a certain electrical conductivity and according to [24] obtaining correct electrical discharges requires setting the appropriate voltage value. In this case, when treating the Ti-6Al-4V alloy with the use of a copper electrode and deionized water as a dielectric, analysis of the relationships and recorded  $U(t)$  and  $I(t)$  waveforms indicates the optimal value for the application of  $U = 100$  V.

The analysis of the influence of the rotational speed of the tool electrode ( $N$ ) showed that the use of a higher value ( $N = 500$  rpm) (Figure 11a) resulted in a higher material removal rate ( $MRR > 10 \mu$ m/s). Higher rotational speeds of the working

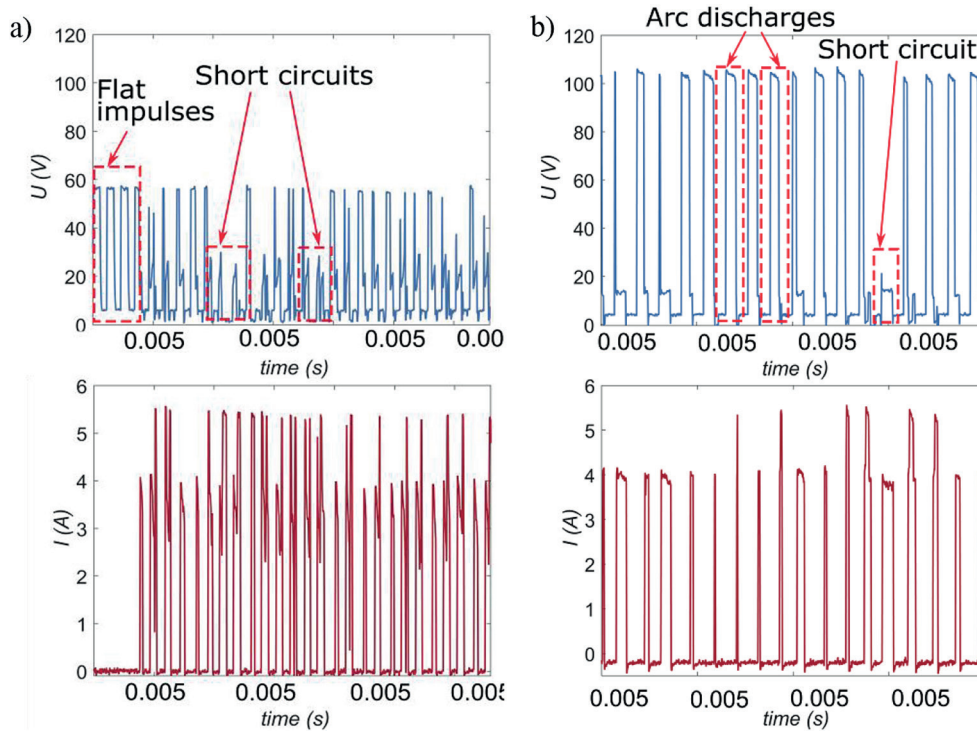


**Figure 9.** The voltage and current waveforms for using of the working voltage: a) 60 V and b) 120 V; constant parameters:  $I = 3.33$  A,  $t_{on} = 550$   $\mu$ s,  $N = 300$  rpm

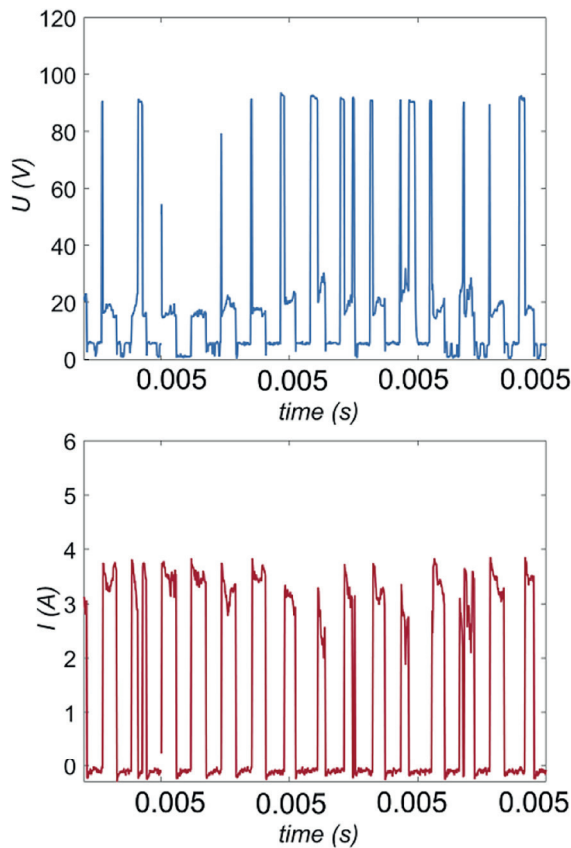


**Figure 10.** The voltage and current waveforms for using of the working voltage 100 V; constant parameters:  $I = 3.33$  A,  $t_{on} = 550$   $\mu$ s,  $N = 300$  rpm

electrode improve the removal of erosion products from the bottom of the hole, which provides greater process stability. This is also confirmed by the results of research by other scientists [25]. During the tests, a ceramic tool guide was used to stabilize the electrode, which eliminated to a minimum possible electrode runout. The drilling test using  $N = 500$  rpm lasted approximately 7 minutes, while the test using  $N = 100$  rpm run for 17 minutes. However, the rotational speed of the working electrode did not significantly affect the linear tool wear and the its values were about 10% (Figure 11b).

#### Effect of EDM parameters on ROC, CYL, ad RLT

For the analysis of the geometry of the drilled holes ROC CYL were selected. In addition, the quality of the drilled holes was examined by analyzing the thickness of the recast layer thickness (RLT). The observation of the holes by scanning electron microscope (SEM) and backscattered electrons (BSE) showed significant differences between the holes including their accuracy and quality.

When selecting the parameters of the EDM-drilling process, an important criteria is to obtain

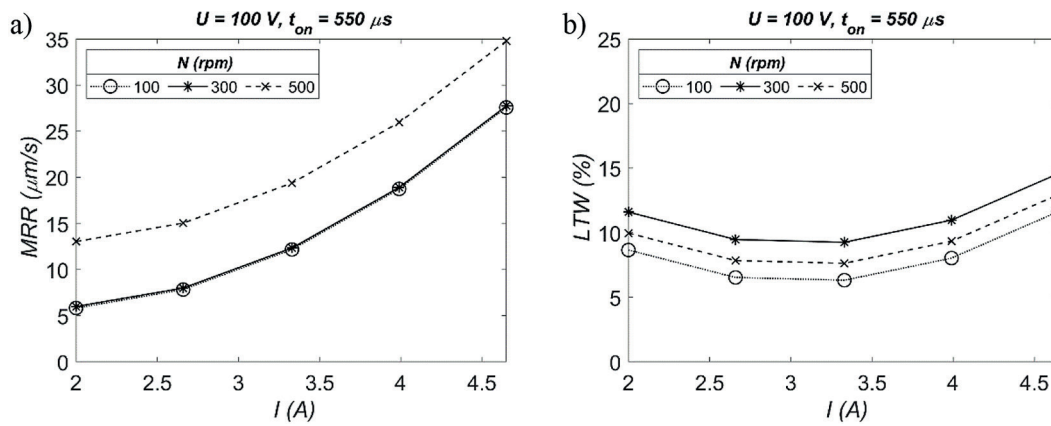


**Figure 11.** Effect of current amplitude ( $I$ ) and electrode rotation ( $N$ ) on: a) material removal rate (MRR) and b) the linear tool wear (LTW)

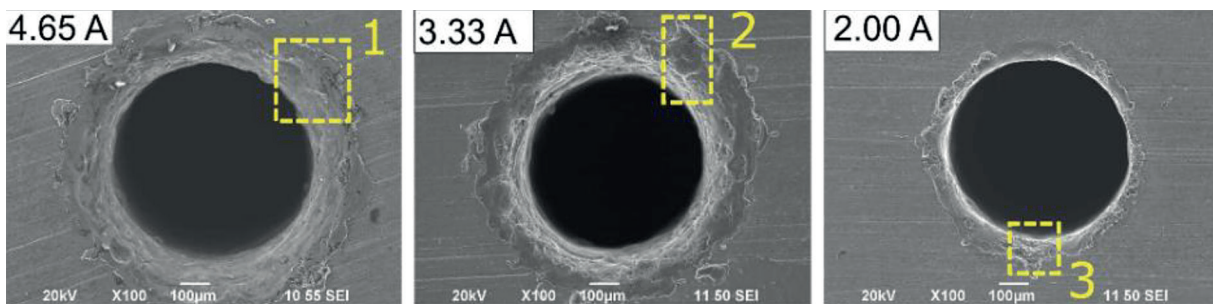


**Figure 12.** SEM graphs of micro-holes for various value of current amplitude;  $t_{on} = 550 \mu\text{s}$ ,  $U = 100 \text{ V}$ ,  $N = 300 \text{ rpm}$

the maximum material removal rate and the minimum tool wear during the process. The previous analysis showed that the use of the current amplitude  $I = 4.65 \text{ A}$  allowed to obtain the highest possible MRR value in these studies. However, the SEM analysis of the quality of the hole drilled with highest value of  $I$  is not satisfactory (Figure 12). At the inlet hole, re-solidified material that has not been fully removed is visible. More re-solidified material at the entrance of the hole was found when the higher  $I$  values ( $\geq 3.33 \text{ A}$ ) were used. When using higher  $I$ , a greater amount of thermal energy transferred in to the workpiece material than when using lower  $I$  values.

An interesting observation was made for higher current amplitude value (4.65 A). The density of microcracks and fractures on the re-solidified material is smaller compared to the holes drilled with smaller values of the current amplitude (2.00 A and 3.33 A) (Figure 14). When using  $I = 4.65 \text{ A}$ , a greater amount of thermal energy transferred into the workpiece material than when using lower  $I$  values. Hence, the temperature of the outermost surface layer could be lower, and the incoming cool fresh liquid did not contribute

to the high temperature difference in the medium. The greater amount of re-solidified material observed and the greater amount of microcracks for the  $I = 4.65 \text{ A}$  used confirm how significant the low thermal conductivity is for the EDM process. And it shows that for these parameters the workpiece was heated deeper. Deeper heat dispersion is also visible by observing the depth of the microcracks. For the highest current value used, the microcracks are less visible in the SEM image. This shows that they are shallower. However, for the applied for the applied  $I = 3.33 \text{ A}$  and  $I = 2.00 \text{ A}$ , they are clearly visible (deeper) and additionally there are fractures (Figure 13).

It is possible that for EDM treatment of a titanium alloy, to sufficiently heat up and remove workpiece material completely even higher current amplitude is needed. This is due to the thermophysical properties of this alloy, which restricts distribution of the thermal energy present in the area of the inter-electrode gap. Proper material removal is largely influenced by the material's ability to absorb and dissipate heat. On the other hand, the Ti-6Al-4V alloy is characterized by a relatively low thermal conductivity and high

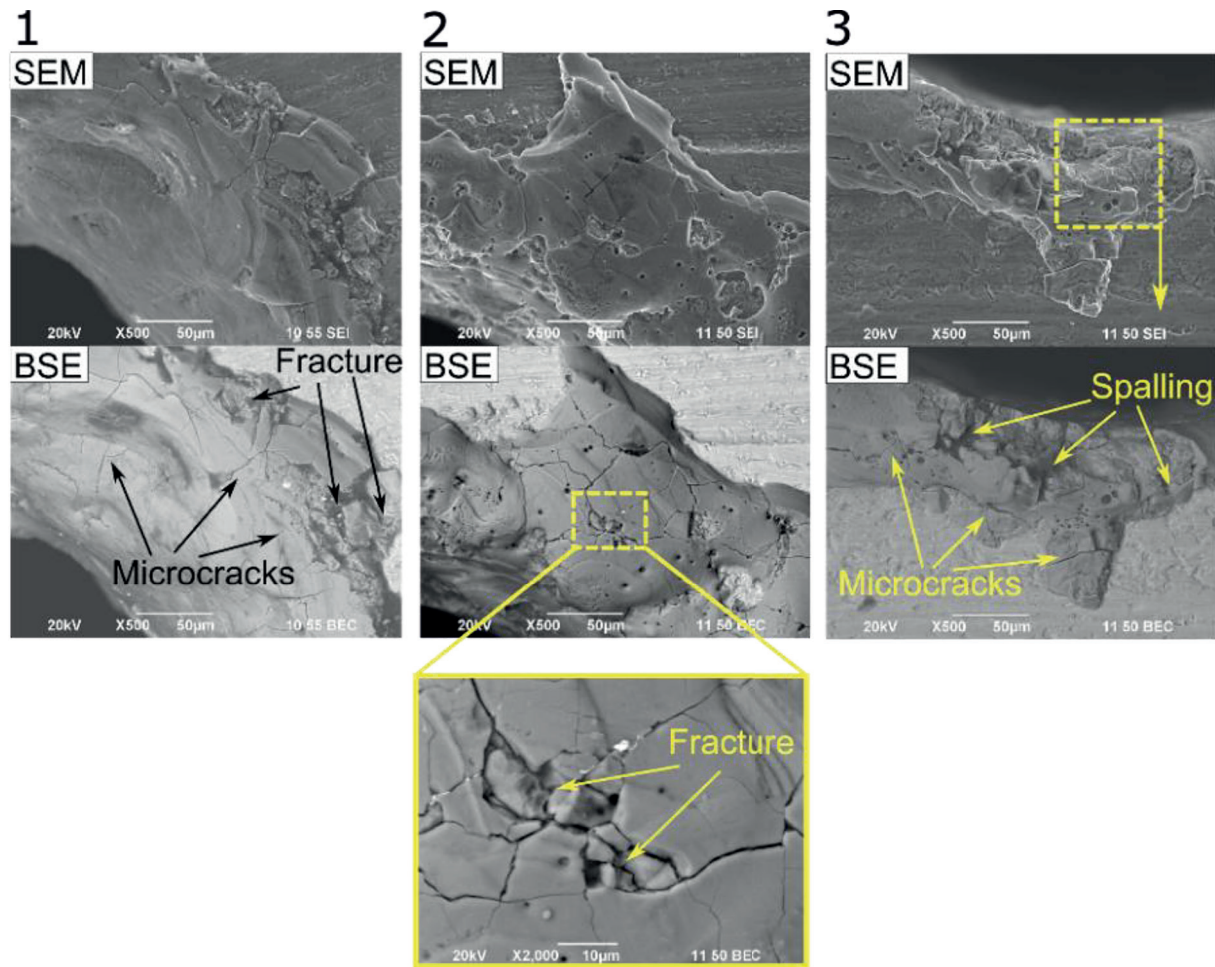


**Figure 13.** Magnification of fragments marked as 1, 2, and 3, respectively, in Figure 10

electrical resistance. Moreover, the melting point of this alloy is increased and amounts to approx. 1650° C [4,26]. These properties of the Ti-6Al-4V alloy cause it difficult to select optimal EDM process parameters ensuring an acceptable accuracy of the geometry of the drilled holes. The layer of re-melted material on the surface around the hole entrance can be removed by grinding operation. However, the entry edge of the hole may remain with poor accuracy.

In addition, SEM analysis showed that a smoother edge of inlet hole was obtained when using a longer pulse time ( $t_{on} = 1000 \mu s$ ) compared to using a shorter pulse time ( $t_{on} = 100 \mu s$ ) (Figure 14). The SEM images of the edge of inlet hole show that the edge of inlet hole when using  $t_{on} = 1000 \mu s$  is smoother and almost without microcracks and fractures. On the other hand, on the edge of the inlet hole, when using  $t_{on} = 100 \mu s$ , fractures were formed, as well as thicker layers of the re-solidified material. Due to the further use of holes (the holes in the turbine blades are involved in their cooling – the coolant flows through them), it is

more desirable to obtain a smooth edge of the hole entrance. Moreover microcracks might reduce material mechanical properties. A smoother entry edge of the entrance will facilitate the inflow and flow of the coolant as well as will support part durability.

The smoother edge obtained for a longer impulse time (1000  $\mu s$ ) could have been influenced by the lower thermal conductivity (6.7 W/mK) and high electrical resistivity (178  $\mu\Omega cm$ ) of the titanium alloy [21]. As a result, the heat could penetrate deeper into the treated surface. Hence, more molten material remains around the hole entrance. However, the deeper heated sink could cause material layer to cool slower. Hence, less microcracks have appeared on re-solidified and it has a more monolithic structure. Here, too, the influence of the thermal properties of the titanium alloy is observed on the re-solidified material, which is visible through the observation of the visibility of the microcracks. For the 1000  $\mu s$  pulse length used, the microcracks are hardly visible in the SEM image (shallower). And for the used  $t_{on} = 100 \mu s$  they are clearly visible (deeper). This

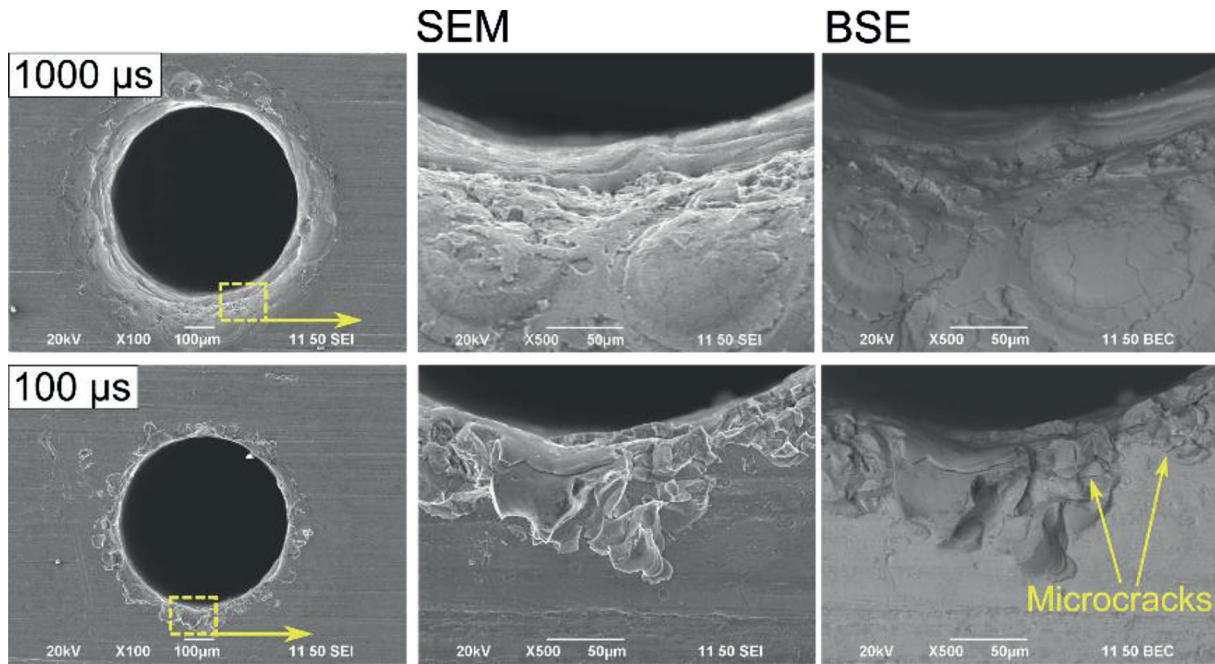


**Figure 14.** SEM and BSE graphs of micro-holes for used time of the impulse: 1000 μs and 100 μs;  $I = 3.33$  A,  $U = 100$  V,  $N = 300$  rpm

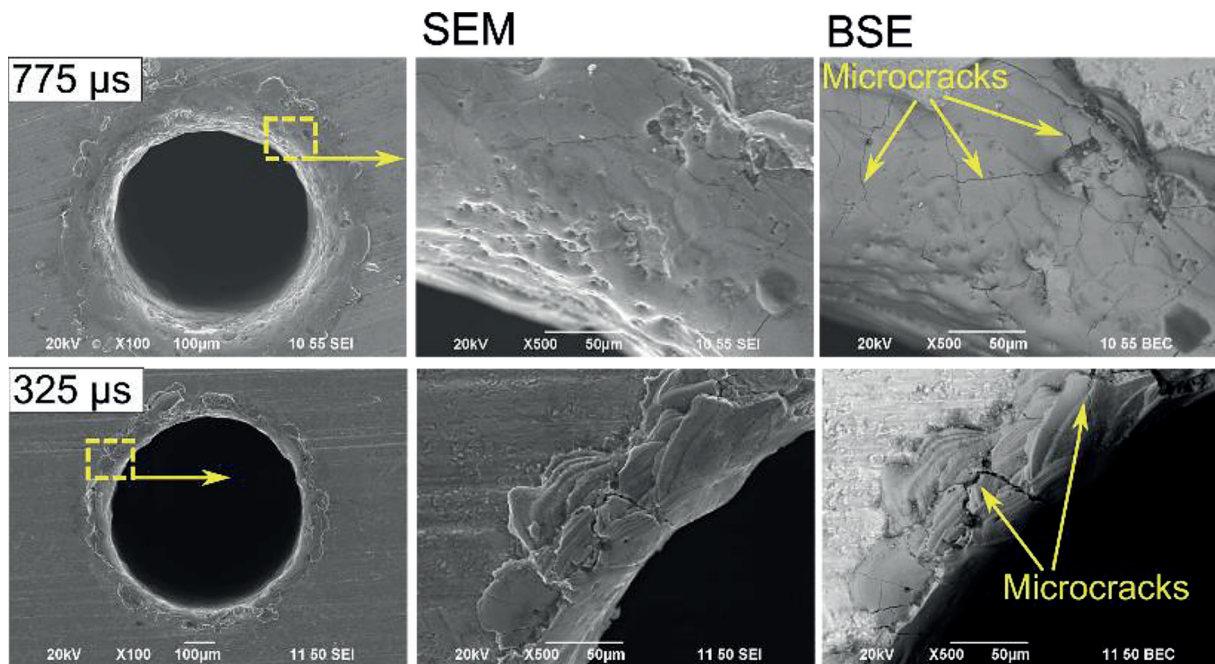


**Figure 15.** SEM and BSE graphs of micro-holes for used time of the impulse: 775 μs and 325 μs;  $I = 3.99$  A,  $U = 100$  V,  $N = 400$  rpm

is important information that shows how much the thermophysical properties of the processed material have an impact on the EDM process.

For other tests, the observation of other SEM and BSE images for the shorter (325 μs) and longer (775 μs) pulse time (Figure 16) shows that the longer pulse time (and also the longer pause time) the better quality of entry of the holes.

In the case of the quality of holes, an important factor is the examination of the obtained re-cast layer. The analysis of the relationships for re-cast layer thickness showed that the length of the pulse time had the greatest influence on its thickness, followed by the rotational speed of the electrode. In the statistical analysis, the "p-value" for these parameters was less than 0.5. On the other

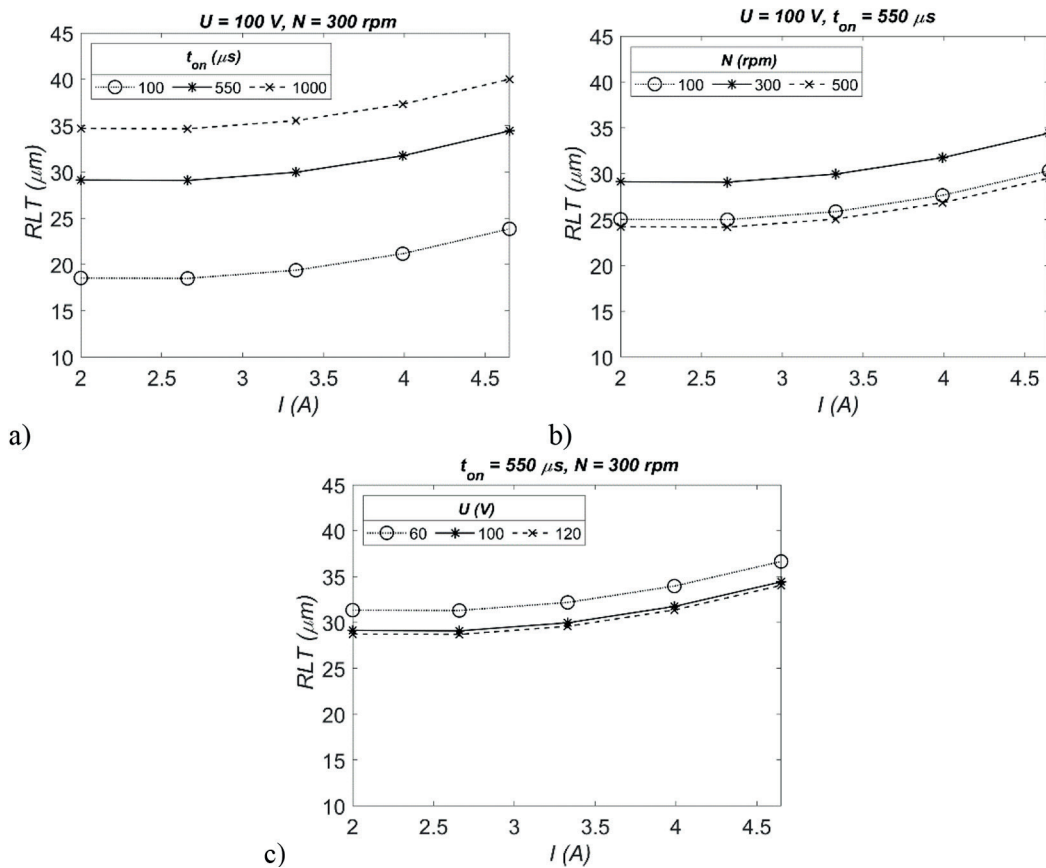


**Figure 16.** Relationship between the recast layer thickness (RLT) and current amplitude ( $I$ ) and: a) time of the impulse ( $t_{on}$ ); b) electrode rotation ( $N$ ); c) open voltage ( $U$ )

hand, the working voltage slightly influenced the thickness of the white layer and for the analyzed values of  $U$ , RLT was approx.  $30\ \mu\text{m}$ . For all analyzed process parameters, the recast layer thickness (RLT) value is in the range of approximately  $20 - 35\ \mu\text{m}$  (Figure 16 a-c). The impact of thermal processes during EDM causes changes in the microstructure of the surface layer of the machined surface, and is the result of the occurrence of defects in it (most often microcracks).

The analysis of the results is in line with the EDM process as much as possible. The length of the pulse time affects the time it takes to supply heat to the treated surface. As a result, the thickest recast layer for the applied value of  $t_{on} = 1000\ \mu\text{s}$  (RLT approx.  $35\ \mu\text{m}$ ) is visible here as well. For the applied extreme values of  $t_{ons}$  ( $100\ \mu\text{s}$  and  $1000\ \mu\text{s}$ , respectively), the observation of SEM images of the white layer shows the presence of microcracks (Figure 17). Microcracks are an

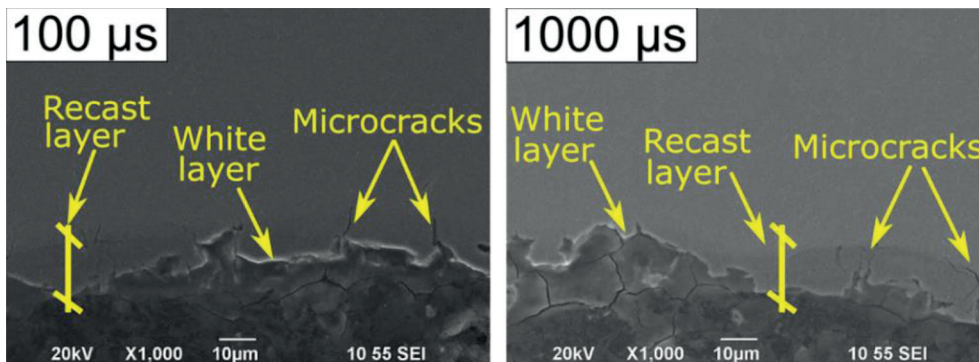


**Figure 17.** SEM graphs of the recast layer thickness for used time of the impulse:  $100\ \mu\text{s}$  and  $1000\ \mu\text{s}$ ;  $I = 3.33\ \text{A}$ ,  $U = 100\ \text{V}$ ,  $N = 300\ \text{rpm}$

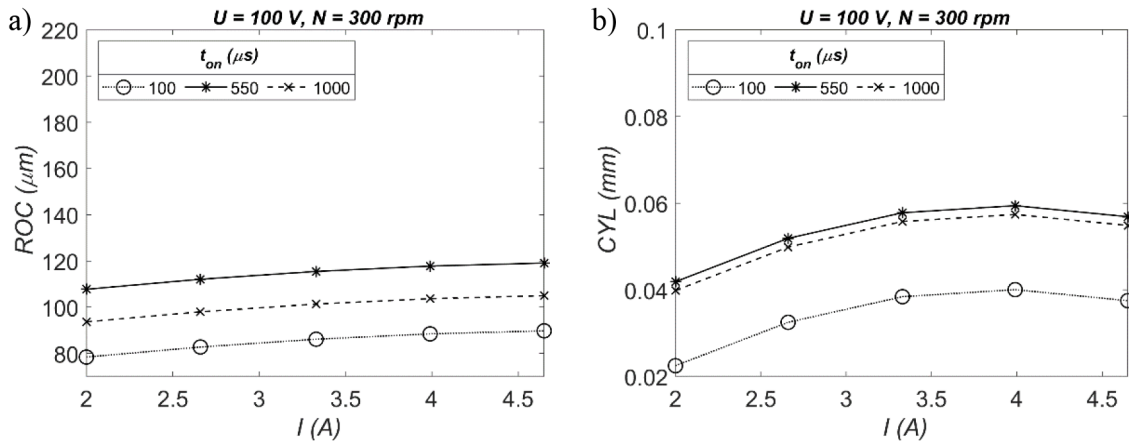


**Figure 18.** Effect of current amplitude ( $I$ ) and pulse on time ( $t_{on}$ ) on: (a) the radial overcut (ROC) and (b) cylindricity (CYL)

undesirable effect and can cause, inter alia, reduction of the fatigue strength of the material [23].

The analysis of the impact of the pulse time on radial overcut (ROC) and cylindricity (CYL) (Figure 18a, Figure 18b, respectively) showed, however, that when using  $t_{on} = 100 \mu\text{s}$ , the values of these result factors were lower. The difference between ROC and CYL when using the maximum and minimum  $t_{on}$  was about 20% for ROC and about 50% for CYL. The inlet edge of the hole, as seen in the images above, is less regular compared to a edge of inlet hole for drilled with the minimum ton value. However, the presence of a significant amount of microcracks and defects sets the quality of this hole at the low level.

The analysis of the influence of the working voltage on radial overcut showed that the lower values of the working voltage (60 V and 100 V) provided lower ROC values (about 100 – 120  $\mu\text{m}$ ) (Figure 19a) than for the applied  $U = 120 \text{ V}$ . For applying values of  $U = 120 \text{ V}$ , the ROC values are

almost twice as large. Using an operating voltage of 120 V could results in overwhelming amount of energy per discharge, and increased amount of removed material. However, such parameter values did not resulted in a significant amount of re-solidified material at the entrance of the hole, which appeared when using  $U = 100 \text{ V}$  and  $U = 60 \text{ V}$ .

By analyzing the radial overcut parameter together with the material removal rate and linear tool rate, it is possible to observe the optimal operating voltage value of 100 V. For this value, the lowest LTW was for the other values of the process parameters used (at the level of approx. 10%, see in Figure 6).

Moreover, the analysis of the influence of the working voltage showed that this parameter slightly influenced the cylindricity values, which for the applied  $U$  values was at the level of about 0.04 mm (Figure 19b).

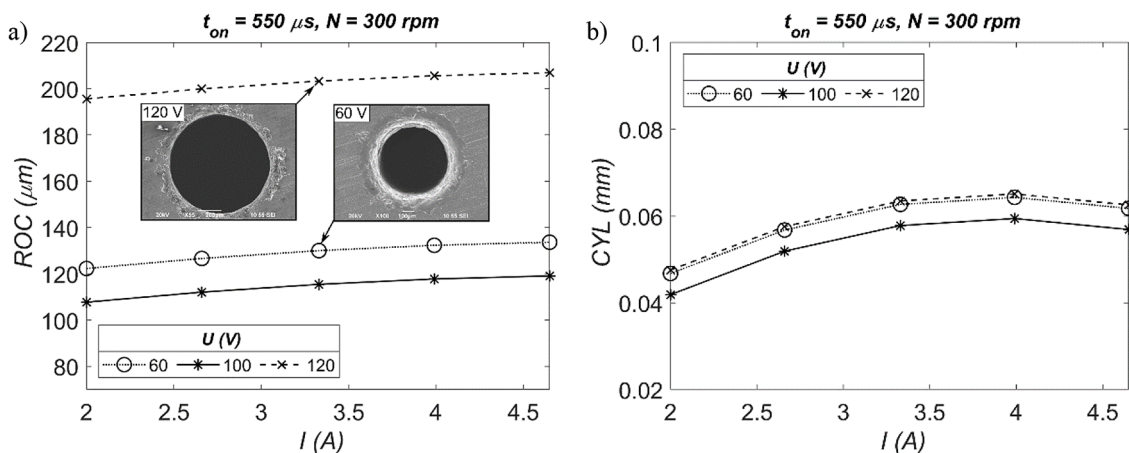


**Figure 19.** Effect of current amplitude ( $I$ ) and open voltage ( $U$ ) on: a) ROC; b) CYL.

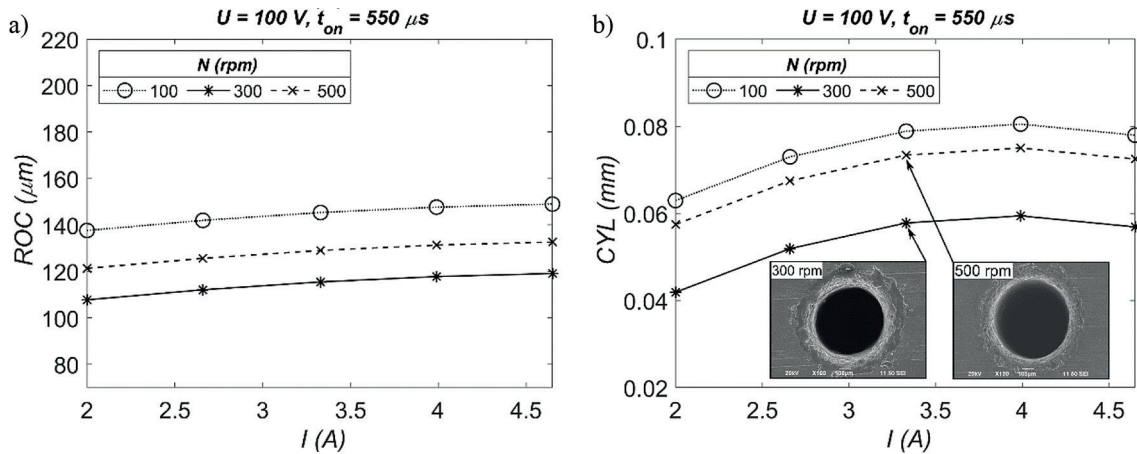


Figure 20. Effect of current amplitude ( $I$ ) and electrode rotation ( $N$ ) on: a) ROC; b) CYL.

Moving on to the analysis of the influence of the rotational speed of the electrode ( $N$ ) on the efficiency factors. The analysis of the MRR relationship ( $I, N$ ) (Figure 11a) showed that the highest MRR values were obtained at  $N = 500$  rpm. But, the analysis of the ROC ( $I, N$ ) and CYL ( $I, N$ ) relationships showed that lower ROC values (about  $100 \mu\text{m}$ ) and also smaller cylindricity values (about  $0.04 \text{ mm}$ ) were obtained when using  $N = 300$  rpm (Figure 20a and Figure 20b, respectively). Taking into account the accuracy of the hole performance and the material removal rate, the optimal value of the working electrode rotation to be used is 300 rpm.

On the other hand, when analyzing the impact of the tool rotation on the recast layer thickness by observing SEM photos, it turned out that the use of the highest and the lowest value of this parameter allowed to obtain a very similar RTL value (at the level of approx.  $25 \mu\text{m}$ , Figure 16b), and for  $N = 300$  rpm approx.  $30 \mu\text{m}$ . This shows that the rotation of the working electrode slightly affects the recast layer thickness factor.

Microcracks were also observed in the thermally changed layer (Figure 21).

The quality of the drilled holes, re-solidified material occurrence at the hole entry, dimensional and shape inaccuracy, can be strongly related to the properties of Ti-6Al-4V titanium alloy, mainly low thermal conductivity and high electric resistance. A key consideration in the material removal process during the EDM is how quickly the heat present in the gap area can be absorbed and dispersed in the workpiece. Therefore, the properties of the Ti-6Al-4V alloy make it difficult for the material to conduct heat. Moreover, once the energy has been absorbed by the workpiece, it is difficult to dissipate heat therein due to the lack of a constant increase in the temperature of the workpiece. This is due to the increase in the electrical resistance of the titanium alloy along with its temperature [4]. Accordingly, the high electrical resistance and low thermal conductivity of the titanium alloy results in appearance of large amount of re-solidified material around the opening of the bore for applied  $I$

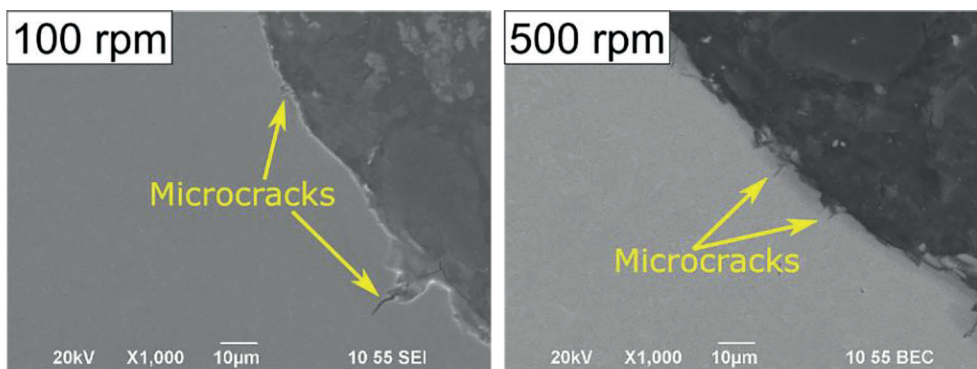


Figure 21. SEM graphs of the recast layer thickness for used the rotational speed of the electrode ( $N$ ): 100 rpm and 500 rpm;  $t_{on} = 550 \mu\text{s}$ ,  $I = 3.33 \text{ A}$ ,  $U = 100 \text{ V}$

> 3.33 A, as well as for the pulse time duration  $\geq 550 \mu\text{s}$ , compared to the use of lower values A and tons. However, observation of the resulting re-solidified material in the area of the hole entrance showed that for these parameters fewer micro-cracks on the re-solidified material layer occurred. For higher values of parameters  $I$  and  $t_{on}$ , the surface layer has been heated deeper and its outermost surface has a lower temperature than in the case of shorter heating (when using  $t_{ons} < 550 \mu\text{s}$ ). Hence, there is a smaller temperature difference at the interface treated surface and a much cooler fresh dielectric fluid. As a result, the stresses are lower and there are fewer micro-cracks in the re-solidified material layer.

## CONCLUSIONS

The article presents an analysis of the results of electrical discharge micro-drilling in the Ti-6Al-4V titanium alloy. Currently, the production of micro-holes in titanium alloys with smaller and smaller diameters (less than 0.5 mm) is popular topic. This is due to the need for continuous improvement of manufacturing processes as well the service life of aircraft engine parts, which are cooled during operation by the flow of the coolant through the micro-holes.

The analysis of the results from the conducted research showed that the Ti-6Al-4V titanium alloy is a difficult-to-machine material for EDM due to its thermophysical properties. The properties of this titanium alloy, such as low thermal conductivity and high electrical resistance, slow down the EDM treatment and contribute to increased wear of the working electrode. Moreover, during the process the workpiece does not heat up well enough, and the heat does not penetrate the material surface sufficiently. This makes the EDM treatment of the Ti-6Al-4V alloy difficult. In addition, analysis of the SEM images showed significant differences in the formation of re-solidified material around the hole entrance (forming micro-cracks and fractures). This gives important information on how much thermophysical properties have an impact on the EDM treatment of a titanium alloy. Also, the quality of the obtained micro-holes is not satisfactory. Below, they are the most important conclusions regarding the analysis of the quality of micro-holes. Observation of the re-solidified material around the inlet port showed that using a larger current amplitude resulted in

fewer microcracks and additionally shallower than when using a current amplitude less than 3.33 A. The time pulse duration parameter had the greatest impact on the recast layer thickness. This is related to the thermophysical properties of the titanium alloy and the heat distribution in the workpiece. The thickness of the recast layer was in the range of 20 – 35  $\mu\text{m}$ . The quality of the micro-holes was significantly influenced by the applied open voltage. The smallest radial overcut (about 100  $\mu\text{m}$ ) and cylindricity (about 0.04 mm) values were obtained for an operating voltage of 100 V. The analysis of the results showed that the highest material removal rate was obtained for the applied value of electrode rotation 500 rpm, however the radial overcut and cylindricity analysis showed that better hole quality was obtained for electrode rotation 300 rpm. Drilling process values are: current amplitude 3.33 – 4.65 A, pulse time duration 550 – 1000  $\mu\text{s}$ , open voltage 100 V, tool rotation speed 300 rpm.

## REFERENCES

1. Shabgard M., Khosrozadeh B. Investigation of carbon nanotube added dielectric on the surface characteristics and machining performance of Ti-6Al-4V alloy in EDM process. *Journal of Manufacturing Processes* 2017; 25: 212–219.
2. Franczyk E., Ślusarczyk Ł., Zębala W. Drilling burr minimization by changing drill geometry. *Materials* 2020; 13(14), 3207.
3. Ezugwu E.O., Wang Z.M. Titanium alloys and their machinability—a review. *Journal of Materials Processing Technology* 1997; 68(3): 262–274.
4. Fonda P., Wang Z., Yamazaki K., Akutsu Y. A fundamental study on Ti-6Al-4V's thermal and electrical properties and their relation to EDM productivity 2008; 202(1–3): 583–589.
5. Arshad R., Mehmood S., Shah M., Imran M., Qayyum F. Effect of distilled water and kerosene as dielectrics on machining rate and surface morphology of Al-6061 during electric discharge machining. *Advances in Science and Technology Research Journal* 2019; 13(3): 162–169.
6. Yilmaz, O., Bozdana, A.T., Okka, M.A. An intelligent and automated system for electrical discharge drilling of aerospace alloys: Inconel 718 and Ti-6Al-4V. *The International Journal of Advanced Manufacturing Technology* 2014; 74: 1323–1336.
7. Natsu W., Maeda H. Realization of high-speed micro EDM for high-aspect-ratio micro hole with mist nozzle. *Procedia CIRP* 2018; 68: 575–577.

8. Skoczypiec S., Ruszaj A. A sequential electrochemical-electrodischarge process for micro part manufacturing. *Precision Engineering* 2014; 38(3): 680–690.
9. Munz M., Risto M., Haas R. Specifics of flushing in electrical discharge drilling. *Procedia CIRP* 2013; 6: 83–88.
10. Machno M., Bogucki R., Szkoda M., Bizoń W. Impact of the deionized water on making high aspect ratio holes in the Inconel 718 Alloy with the use of electrical discharge drilling. *Materials* 2020; 13(6), 1476.
11. Bassoli, E., Denti, L., Gatto, A., Luliano L. Influence of electrode size and geometry in electro-discharge drilling of Inconel 718. *The International Journal of Advanced Manufacturing Technology* 2016; 86, 2329–2337.
12. Abu Qudeiri J.E., Mourad A.-H.I., Ziout A., Haider Abidi M., Elkaseer A. Electric discharge machining of titanium and its alloys: review. *The International Journal of Advanced Manufacturing Technology* 2018; 96: 1319–1339.
13. Kumar M., Datta S., Kumar R. Electro-discharge Machining Performance of Ti–6Al–4V Alloy: Studies on Parametric Effect and Phenomenon of Electrode Wear 2019; 44: 1553–1568.
14. Wang X., Liu Z., Xue R., Tian Z., Huang Y. Research on the influence of dielectric characteristics on the EDM of titanium alloy. *The International Journal of Advanced Manufacturing Technology* 2014; 72: 979–987.
15. Gosavi Vaibhav Y., Phafat Nitin G. Analysis of the influence of EDM parameters in micro hole drilling of titanium wrought alloy, *International Journal of Materials Science and Engineering* 2016; 4(1): 34–35.
16. Dewangan S., Deepak Kumar S., Jha Kumar S., Kumar Biswas Ch. Optimization of micro-EDM drilling parameters of Ti–6Al–4V alloy. *Materials Today: Proceedings* 2020; 33(8): 5481–5485.
17. Tiwary, A.P., Pradhan, B.B., Bhattacharyya, B. Investigation on the effect of dielectrics during micro-electro-discharge machining of Ti-6Al-4V. *The International Journal of Advanced Manufacturing Technology* 2018; 95: 861–874.
18. Rajamanickam S., Prasanna J. High aspect ratio small hole electric discharge drilling (EDD) of superalloys: Inconel 718 and Ti-6Al-4V review paper. *International Journal of Pure and Applied Mathematics* 2018; 119(16): 1637–1642.
19. Ram Prasad A.V.S., Ramji K., Datta G.L., An experimental study of wire EDM on Ti-6Al-4V. *Procedia Materials Science* 2014; 5: 2567–2576.
20. Kuppan, P.; Narayanan, S.; Oyyaravelu, R.; Balan, A.S.S. Performance evaluation of electrode materials in electric discharge deep hole drilling of Inconel 718 superalloy. *Procedia Engineering* 2017; 174: 53–59.
21. Khosrozadeh, B., Shabgard, M. Effects of hybrid electrical discharge machining processes on surface integrity and residual stresses of Ti-6Al-4V titanium alloy. *The International Journal of Advanced Manufacturing Technology* 2017; 93: 1999–2011.
22. Gulbinowicz Z., Gorocho O. J. Skoczylas P. Mathematical modeling of material erosion during the electrical discharge. *Advances Science and Technology Research Journal* 2020; 14(2): 27–33.
23. Świercz R., Oniszek-Świercz D., Chmielewski T. Multi-Response optimization of electrical discharge machining using the desirability function. *Micromachines* 2019; 10(1), 72.
24. Basak I., Ghosh A. Mechanism of spark generation during electrochemical discharge machining: a theoretical model and experimental verification. *Journal of Materials Processing Technology* 1996; 62: 46–53.
25. Ekmekci B., Sayar A. Debris and consequences in micro electric discharge machining of micro-holes. *International Journal of Machine Tools and Manufacture* 2013; 65: 58–67.
26. Kibria, G., Sarkar, B.R., Pradhan, B.B., Bhattacharyya B.. Comparative study of different dielectrics for micro-EDM performance during microhole machining of Ti-6Al-4V alloy. *The International Journal of Advanced Manufacturing Technology* 2010; 48: 557–570.